Current changes in tropical precipitation

Richard P. Allan[1], **Brian J. Soden**[2], **Viju O. John**[3], **William Ingram**[3,4], **Peter Good**[3]

[1] Department of Meteorology, University of Reading, Berks, RG6 6AL
[2] RSMAS, Miami, USA
[3] Met Office, Exeter, UK
[4] Department of Physics, University of Oxford, UK

E-mail: `r.p.allan@reading.ac.uk`

Abstract. Current changes in tropical precipitation from satellite data and climate models are assessed. Wet and dry regions of the tropics are defined as the highest 30% and lowest 70% of monthly precipitation values. Observed tropical ocean trends in the wet regime (1.8%/decade) and the dry regions (−2.6%/decade) for the Global Precipitation Climatology Project (GPCP) over the period including Special Sensor Microwave Imager (SSM/I) data (1988-2008) are of smaller magnitude than when including the entire time-series (1979-2008) and in closer agreement with model simulations than previous comparisons. Analysing changes in extreme precipitation using daily data within the wet regions we find an increase in the frequency of the heaviest 6% of events with warming for the SSM/I observations and model ensemble mean. The SSM/I data indicates an increased frequency of the heaviest 0.2% of events of approximately 60% per K warming. This is larger than expected from the Clausius Clapeyron response and at the upper limit of the model simulations which display a substantial range in responses.

1. Introduction

Substantial changes in the global water cycle are an expected consequence of a warming climate; this is based upon understanding of the governing physical processes and projections made by sophisticated models of the Earth's climate system (Allen & Ingram 2002). Monitoring changes in tropical precipitation is a vital step toward building confidence in regional and large-scale climate predictions and the associated impacts on society (Meehl et al. 2007).

A number of robust large-scale responses of the hydrological cycle have been identified in models (Held & Soden 2006), relating primarily to increases in low-level moisture with temperature, a consequence of the Clausius-Clapeyron equation. Moisture increases are also thought to lead to the intensification of extreme precipitation (Pall et al. 2007), though sensitivity to model-dependent changes in vertical motion is evident (O'Gorman & Schneider 2009, Gastineau & Soden 2009). Projected rises in global mean precipitation are constrained by radiative-convective balance (e.g. Lambert &

Webb 2008) and increase more slowly than atmospheric moisture. Consequences of increased low-level moisture, enhanced horizontal moisture fluxes and the contrasting changes in mean and extreme precipitation include reductions in the strength of the Walker circulation (Vecchi et al. 2006) and an amplification of global precipitation minus evaporation patterns (Held & Soden 2006), with wet regions becoming wetter at the expense of dry regions (Chou et al. 2007); many of these anticipated responses have been known about for some time (Mitchell et al. 1987).

Improving confidence in climate projections demands the use of observations, sampling the many aspects of the global energy and water cycles, to evaluate the relevant processes simulated by models. It is important to establish causes of disagreement, for example relating to observing system deficiencies or inadequate representation of forcing and feedback processes in models. There is observational evidence of increased tropical monthly-average moisture and precipitation (Wentz et al. 2007) and an amplification of extreme precipitation events in response to atmospheric warming (Lenderink & van Meijgaard 2008, Allan & Soden 2008) as well as a contrasting precipitation response over wet and dry regions of the tropics (Zhang et al. 2007, Allan & Soden 2007, Chou et al. 2007). While observed precipitation responses appear larger than those simulated by models (Zhang et al. 2007, Wentz et al. 2007, Allan & Soden 2008) it is unclear whether this relates to model deficiency, inadequacy in the observing system or is a statistical artifact of the relatively short satellite record (Liepert & Previdi 2009). The aim of the present work is to identify physically understandable, robust responses of tropical precipitation and highlight discrepancies relating to limitations of the observing system or the model simulations. We update and extend analysis of current changes in tropical precipitation and its extremes, addressing the questions: (1) What are current trends in tropical mean precipitation? (2) Are the wet regions becoming wetter at the expense of the dry regions? (3) Is there an intensification in extreme precipitation with warming in models and observations over the period 1979-2008?

2. Current changes in tropical precipitation

Increases in tropical (30°S-30°N) precipitation since 1979 have been detected using observational datasets (Wentz et al. 2007, Adler et al. 2008), in particular for the oceans and over ascending branches of the large-scale circulation (Allan & Soden 2007). The observed responses appear more pronounced than simulations made using coupled atmosphere-ocean climate models with realistic radiative forcings from the phase 3 of the Coupled Model Inter-comparison Project (CMIP3) and also atmosphere-only experiments (AMIP3) forced with observed sea surface temperature (SST) and sea ice (Wentz et al. 2007, Allan & Soden 2007) although the results are highly sensitive to the time period and dataset used (John et al. 2009, Liepert & Previdi 2009).

A critical issue with regard to observing current changes in precipitation is the limitations in the satellite datasets. The Global Precipitation Climatology Project (GPCP; Adler et al. 2008) incorporates a blend of satellite infra-red radiances and

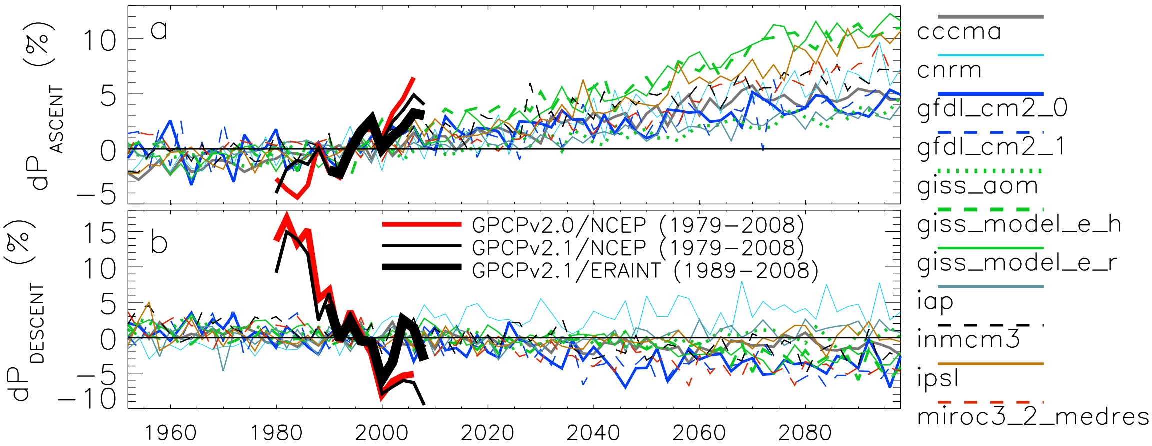

Figure 1. Precipitation anomalies (2-year averages) relative to the mean for the 1989-1999 period over (a) ascending and (b) descending branches of the tropical circulation for CMIP3 coupled atmosphere-ocean models and versions 2.0 and 2.1 GPCP observations applying NCEP or ERA Interim reanalysis vertical motion fields. Updated from Allan & Soden (2007).

predominantly land-based rain gauges since 1979 with microwave ocean measurments from the Special Sensor Microwave Imager (SSM/I) since 1988. In addition to GPCP we also consider the SSM/I-only ocean product (version 6) developed by Wentz et al. (2007) using the satellite series: F08 (1987-1991), F11(1992-1999) and F13 (2000-2008). It is important to note the different sources that contribute to precipitation estimation over land and ocean. In addition, changes in the coverage and calibration issues limit the accuracy in these datasets, in particular for identifying decadal changes. Also critical are the known differences between the satellite datasets and model simulations in representing the probability distribution of precipitation events (Wilcox & Donner 2007, Field & Shutts 2009). While limitations apply both to the models and observations, it is of considerable value to identify physically understandable, robust responses of the tropical water cycle.

2.1. Ascending and Descending Regimes

Fig. 1 shows precipitation anomalies in ascending and descending branches of the tropical circulation, using 500 hPa vertical motion fields from atmospheric reanalyses to sub-sample the observed precipitation and model vertical motion to sample model precipitation. The comparison is identical to Allan & Soden (2007) but also displays an updated version (v2.1) of the GPCP dataset and also uses European Centre for Medium-range Weather Forecast (ECMWF) Interim reanalysis (ERA Interim) data, based upon Uppala et al. (2005), in place of National Center for Environmental Prediction reanalysis 1 (NCEP; Kalnay et al. 1996). The update from GPCP version 2.0 to 2.1 does not alter trends substantially. However, using ERA Interim data reduces the magnitudes of trends, in closer agreement with the models. We propose that the NCEP reanalysis is particularly sensitive to improved representation of vertical motion, with reduced misclassification of GPCP precipitation events in descent regions over time, that may appear to enhance precipitation trends. Regardless, the sensitivity of precipitation trends to reanalysis vertical motion fields motivate an alternative approach.

2.2. Wet and Dry Regimes

To avoid the use of reanalysis fields, instead percentile bins of precipitation were used to define the wettest and driest regions. Monthly precipitation values were sorted by intensity, including dry grid-points. Mean precipitation was calculated for the the driest 50% of grid boxes and subsequently for each 10% bin ranging from 50-60% up to the wettest 10% of grid-boxes. Monthly area-weighted means were computed over each bin for the GPCP v2.1 data (1979-2008) and also for "run1" of all AMIP3 models which spanned the entire period 1979-2001: CNRM-CM3, GISS-E-R, INMCM3, IPSL-CM4, MIROC3.2-hires, MIROC3.2-medres, MRI-CGCM2-3.2a, NCAR-CCSM3, HadGEM1 (obtained from www-pcmdi.llnl.gov) and a model ensemble mean. The resulting time-series were deseasonalized to reduce the influence of the large changes in solar forcing and associated circulation shifts that may not be a good surrogate for climate change. Circulation changes are also associated with El Niño although sampling wet or dry regimes will reduce the impact of these changes somewhat. Precipitation trends were calculated using linear least-squares fits. Essentially we seek to quantify the statistical distribution of tropical precipitation and its linear change with time.

Figure 2 shows trends and associated correlation (r) for each percentile bin for the GPCP data, considering the entire period and the 1988-2008 period, which included SSM/I ocean data. Also shown are trends for the model ensemble mean and range for the 9 individual models (grey shading); the ensemble mean correlation coefficient does not lie entirely within the inter-model spread since forming an ensemble can increase correlation as the random unforced component of variability is reduced. Trend magnitudes for GPCP are reduced when excluding the pre-SSM/I period (1979-1987) from the analysis, in closer agreement with the model results. Caution in using pre-1988 GPCP data has been expressed previously (e.g. Adler et al. 2008) due to issues with inter-calibration of the infra-red satellite radiances and homogeneity associated with changes from infra-red-only to combined infra-red and microwave ocean precipitation retrievals.

Fig. 2 shows a clear partition between positive trends above the 60-70th percentile and negative trends below these percentiles for the GPCP and model data. Pall et al. (2007) found this partition to be sensitive to the latitude chosen, being closer to the 90th percentile for the global mean, although they considered daily model data at approximately 2.7 times CO_2 levels relative to a control. Guided by Fig. 2, wet and dry regions of the tropics were defined as the driest 70% and wettest 30% of grid-boxes for each model and satellite dataset. Time series were calculated for these regimes over the entire tropics and for land and ocean regions separately.

Figure 3 displays deseasonalized tropical ocean anomalies of SST (HadISST; Rayner

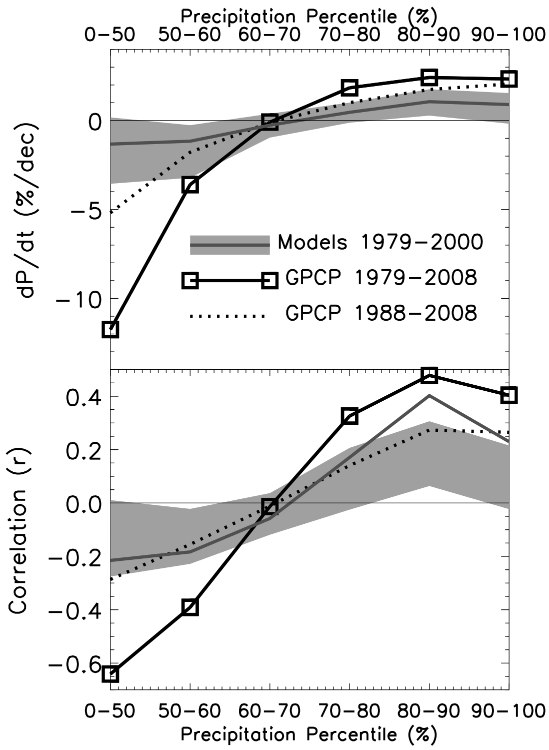

Figure 2. (a) Linear trends in precipitation with time (dP/dt in %/decade) and (b) associated correlation coefficient, r, with percentile bins of tropical monthly precipitation for GPCP data, AMIP3 model ensemble mean and the range for individual models (grey shading).

et al. 2003) and precipitation and the wet and dry region precipitation time series for models, GPCP and SSM/I. Linear trends and correlation between precipitation and SST are presented in Table 1; a two-tailed t-test, allowing for autocorrelation (Yang & Tung 1998), was employed to detect significant correlation at the 95% confidence level. Positive precipitation anomalies coincide with warm El Niño years in the models and observations, attributable to the wet tropical region response (Fig. 3c). This relationship is statistically significant with mean precipitation anomalies for GPCP and the model ensemble mean increasing at around 6-10%K^{-1} depending upon the time period, close to the Clausius-Clapeyron rate, with a spread across the models of 2.9-11%K^{-1} (Table 1). The SSM/I data show a response around twice as large as for GPCP.

Over the tropical oceans, positive precipitation trends are apparent for the wet region (Fig. 3c) and negative trends in the dry regions (Fig. 3d), consistent with Allan & Soden (2007), despite a differing methodology. Observed wet region trends range from 1.8-3.0%/decade, overlapping with the upper range of the inter-model spread. The model ensemble trend is also positive, but smaller (1%/decade).

Negative trends in the dry regions for GPCP data are more than halved when excluding the pre-SSM/I period. GPCP anomalies are substantially more positive than model anomalies during 1981-82 and 1984-86, and further analysis is required to assess

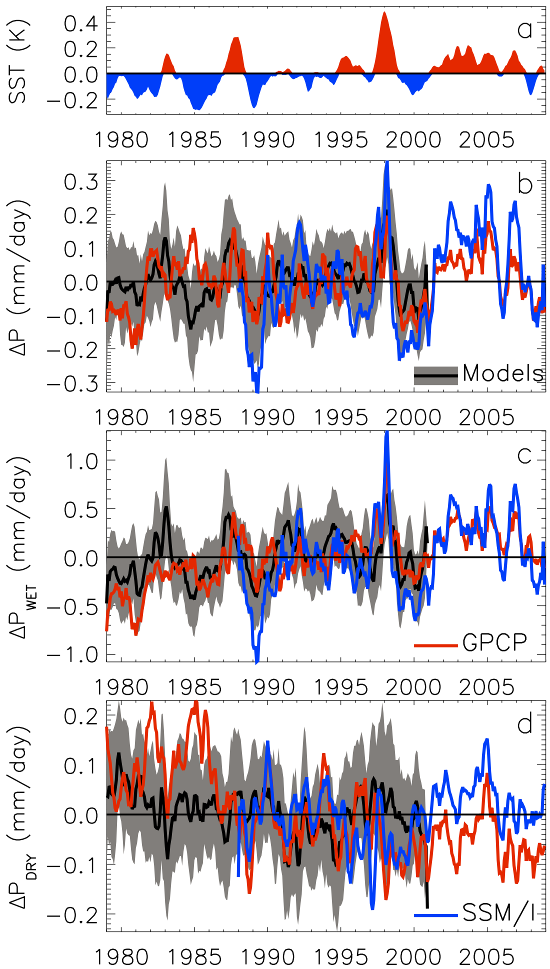

Figure 3. Anomalies of (a) sea surface temperature (SST) and (b) precipitation (P), partitioned into (c) wet and (d) dry regions of the tropical oceans for observations and models (grey shading denotes ± 1 standard deviation).

the accuracy of GPCP data during these periods (Adler et al. 2008). Nevertheless, GPCP ocean trends for the 1988-2008 period are twice the model ensemble mean trends for the 1979-2001 period despite similar observed SST trends for the two periods (0.06 and 0.08 $K/decade$ respectively). SSM/I data do not show a statistically significant trend, partly due to positive anomalies since 2000, at odds with the GPCP data. This coincides with the switch between F11 and F13 satellites in the record and may therefore be an inter-calibration issue. Trends over tropical land regions are generally not statistically significant apart from GPCP for the wet regions over the period 1988-2008.

For wet regions over the entire tropics, there is a positive trend of 1.9% per decade for 1988-2008 GPCP data, around double the model ensemble mean trend for 1979-2001. For the NCEP tropical surface temperature trend over 1988-2008 (0.12 $K/decade$) this corresponds to a sensitivity of 16%/K for GPCP, above that expected from Clausius-

Table 1. Linear trends in precipitation (P) and regression with sea surface temperature (SST) for models and observations over tropical land and ocean for wet and dry regimes. * denotes significant correlation at the 95% confidence interval.

Dataset	Period	Tropics	Tropical Wet	Tropical Dry
		Interannual relationships: dP/dSST (%/K), Ocean		
GPCP v2.1	1979-2008	$6.4\pm1.4^*$	$15.5\pm1.7^*$	$-20.3\pm3.2^*$
GPCP v2.1	1988-2008	$9.8\pm1.8^*$	$13.3\pm2.1^*$	-2.3 ± 3.6
SSM/I v6	1988-2008	$21.6\pm2.5^*$	$23.1\pm2.7^*$	6.1 ± 6.8
Models (range)	1979-2000	$7.7\pm0.5^*$ (+2.9-+11)	$10.1\pm1^*$ (+5.6-+14)	1.8 ± 1.3 (−5.3-+10)
		Trends: dP/dt (%/decade), Land+Ocean		
GPCP v2.1	1979-2008	0.5 ± 0.2	$2.2\pm0.2^*$	$-4.7\pm0.4^*$
GPCP v2.1	1988-2008	$1.0\pm0.3^*$	$1.9\pm0.4^*$	-2.1 ± 0.7
Models (range)	1979-2000	$0.4\pm0.1^*$ (−0.4-+0.7)	$0.9\pm0.1^*$ (−0.0-+1.4)	-0.9 ± 0.3 (−2.2-+0.1)
		Ocean		
GPCP v2.1	1979-2008	0.5 ± 0.3	$2.8\pm0.3^*$	$-5.9\pm0.5^*$
GPCP v2.1	1988-2008	0.7 ± 0.4	$1.8\pm0.5^*$	$-2.6\pm0.8^*$
SSM/I v6	1988-2008	$2.8\pm0.7^*$	$3.0\pm0.7^*$	2.6 ± 1.6
Models (range)	1979-2000	0.3 ± 0.2 (−0.8-+1.1)	1.0 ± 0.3 (−0.4-+1.8)	$-1.3\pm0.3^*$ (−2.0-−0.7)
		Land		
GPCP v2.1	1979-2008	0.5 ± 0.4	0.7 ± 0.3	-0.6 ± 0.7
GPCP v2.1	1988-2008	1.7 ± 0.6	$2.2\pm0.6^*$	-0.6 ± 1.3
Models (range)	1979-2000	0.7 ± 0.4 (−1.0-+2.1)	0.5 ± 0.3 (−0.9-+1.6)	1.0 ± 0.7 (−1.9-+3.8)

Clapeyron. It is not clear if this super-Clausius Clapeyron response, also noted elsewhere (Lenderink & van Meijgaard 2008, Liu et al. 2009) has a physical explanation or whether it is a statistical artefact of the limited observational record (Liepert & Previdi 2009); this is discussed further in Section 4.

3. Precipitation Extremes in the Tropical Ocean Wet Region

We now examine in more detail the wet region precipitation response, using daily data from SSM/I and the models. SSM/I 0.25x0.25° data were averaged to a 1×1° grid where at least 50% of grid-point data were valid. Ascending and descending satellite over-passes were combined to provide daily estimates. A 2.5×2.5° product was generated using bi-linear interpolation, consistent with the climate models which were also interpolated to this common grid.

Allan & Soden (2008) excluded dry grid boxes from analysis of daily rainfall intensity. Since ∼70% of the SSM/I grid-boxes were found to be dry while in some models all grid boxes contained at least light rainfall, this potentially causes a substantial sampling disparity. Therefore in the present analysis we consider the wettest 20% of all tropical ocean values, including dry grid-boxes, in the models and SSM/I data.

The method of Allan & Soden (2008) was applied to calculate monthly percentage anomalies in the frequency of rainfall events in each bin, the bin boundaries calculated for one year of data from 1990. Each time-series is deseasonalized with respect to the mean frequency for each month. This is conducted separately for each SSM/I satellite (F08, F11, F13) to avoid satellite inter-calibration issues and to concentrate on interannual anomalies. Results are not substantially altered when considering all satellites as a single record. The calculations are applied to each model (listed in Fig. 4f) separately and averaged to create an ensemble mean (Fig.4c). Also included is a Clausius-Clapeyron experiment where 12 months of SSM/I daily precipitation data for 1990 were perturbed by 7% per K anomaly in observed local SST (HadISST).

There is a correspondence between warm El Niño years (Fig. 4a) and a greater frequency of the heaviest rain (wettest 6% of events) in the observations (b) and the model ensemble mean (c). This relationship is partially explained by the simple Clausius-Clapeyron scaling calculated in Fig. 4d. However, details of the variation differ between the models and observations: there is a strong anti-correlation ($r = -0.78$) between the frequency of 98-100th percentile and 80-86th percentile rainfall in the models, consistent with (Pall et al. 2007), while the observed relationship is more complex.

In agreement with Allan & Soden (2008), the observed response of intense rainfall frequency to warming is 2-3 times larger than the model ensemble mean sensitivity and the response expected from Clausius Clapeyron (Fig. 4e). The model spread for the most intense rainfall bin is substantial (Fig. 4f), ranging from negative to strongly positive, as noted recently (O'Gorman & Schneider 2009, Gastineau & Soden 2009). Specifically, the CNRM, INMCM, IPSL and MIROC models analysed in the present study appear to capture the observed response of around a 60% increase in the frequency of the wettest 0.2% of events per K warming, while the remaining models do not. Turner & Slingo (2009) found that coupled models (CMIP3) using variants of the Arawaka-Schubert convective parametrization (e.g. CGCM, GFDL, MIROC) tend to produce super-thermodynamic responses of precipitation intensity to warming over India at the time of CO_2 doubling; this is not apparent from the AMIP3 simulations considered in the present study.

Using the SSM/I daily precipitation, it is also interesting to ask, how much of the tropical ocean rainfall variability in Fig. 3b is determined by the heaviest daily rainfall events? To address this, we first verified that re-calculate monthly rainfall from the daily data reproduced the monthly products. Linear fits were calculated between the reconstructed monthly precipitation anomalies (P) and perturbed anomalies (P_z) constructed by setting precipitation to zero below each percentile theshold, z. The resulting relationship, $P_{z>94\%}$=0.96P (r = 0.99), demonstrates the dominance of the heaviest rainfall events measured by SSM/I in determining monthly precipitation variation. Rainfall events above the 99th percentile yield the relationship, $P_{z>99\%}$=0.66P, suggesting that the heaviest 1% of rainfall events contribute to around one third of the tropical ocean precipitation anomalies in the SSM/I data.

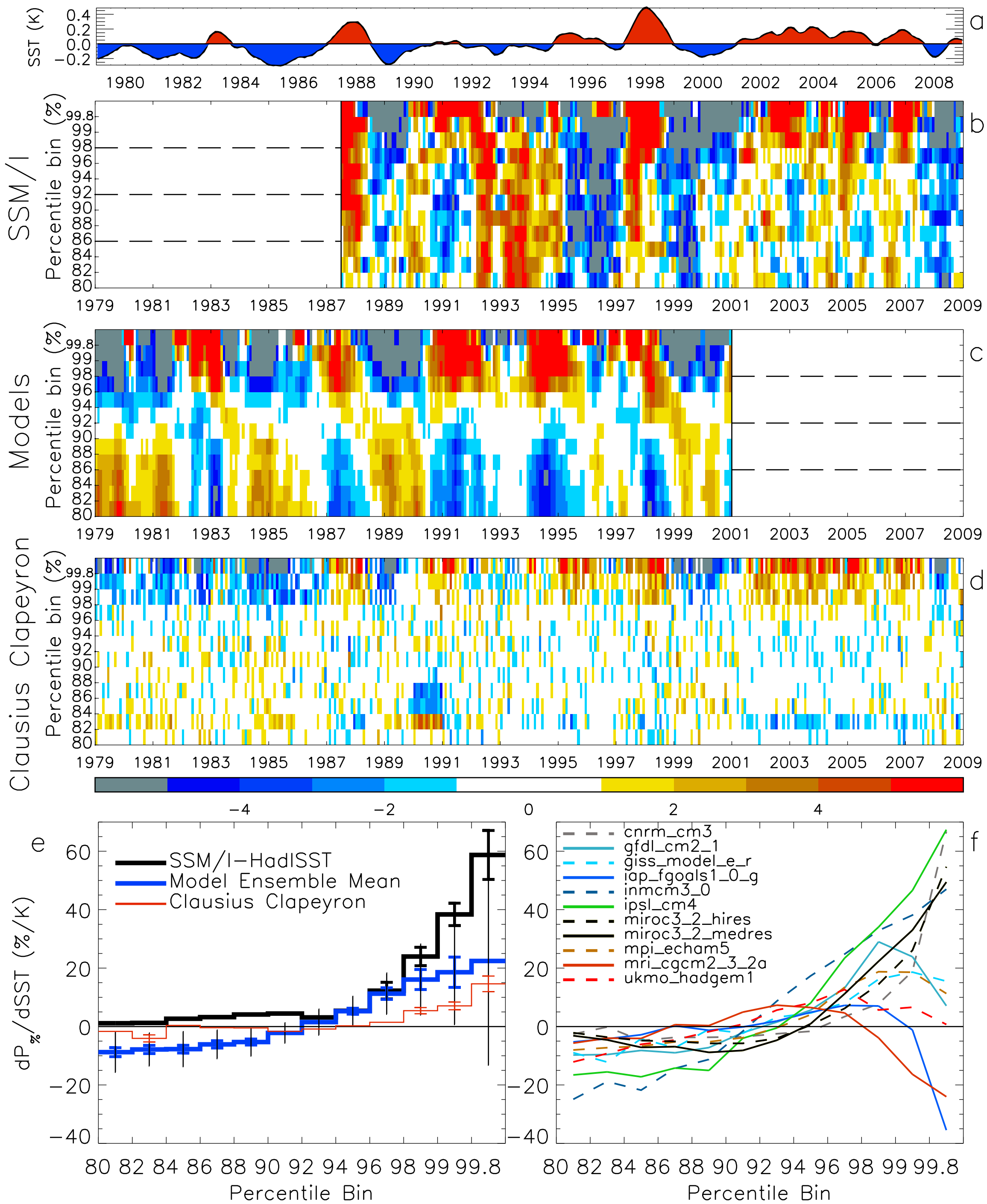

Figure 4. Interannual anomalies (smoothed by ±2 months) of (a) observed SST (HadISST) and the frequency of daily rainfall in percentile bins of intensity ($P_{\%}$) for (b) SSM/I, (c) model ensemble mean and (d) Clausius-Clapeyron estimates based upon SSM/I data for 1990 perturbed by 7% per K observed local SST anomaly. The linear sensitivity of frequency of rainfall intensity to SST change is shown for (e) SSM/I and HadISST, the model ensemble mean and the Clausius-Clapeyron experiment and (f) individual models. In e, standard error bars for the linear fit are plotted where correlation is significant; ± 2 standard deviations are plotted for the model data to denote the model spread.

4. Conclusions

Tropical precipitation variation is quantified for observations and climate model simulations over the period 1979-2008. The wettest 30% of grid-points and the remaining driest regions are sampled separately. Increased precipitation coincides with warm months associated with El Niño. This is attributable to the wet regions of the tropical ocean with observed precipitation increasing at the rate 13.3-15.5 %/K for GPCP data, at the higher end of the model range (5.6-14.0%/K) but lower than SSM/I-only data (23.1%/K). In the SSM/I data, essentially all of the variability in mean tropical ocean precipitation is explained by daily rainfall events above the 94th percentile.

Positive trends in wet regions of the tropical ocean for GPCP are reduced from 2.8%/decade for 1979-2008 to 1.8%/decade for the 1988-2008 SSM/I period, at the upper end of the model range but smaller than SSM/I-only trends. Negative trends in the dry regions of the tropical ocean are detected for the GPCP data and the models. Again GPCP trend magnitudes are reduced when considering the SSM/I period but are still double the model ensemble mean trend of -1.3%/decade. Discrepancy between observed dry-region anomalies since 2000 appears to relate to inhomogeneity of the SSM/I time series. Variation in GPCP precipitation prior to the SSM/I period is also questionable (Adler et al. 2008) and trends over tropical land are not coherent amongst datasets.

Analysing daily precipitation from SSM/I and model simulations for the wettest 20% of ocean grid-boxes demonstrates a clear increase in the frequency of the heaviest rainfall events with warming, consistent with previous analysis (Allan & Soden 2008). The observed frequency of the heaviest 0.2% of rainfall events (including dry grid-points) rises by about 60% per K of warming. This rise is faster than expected from Clausius-Clapeyron, a result also suggested by Lenderink & van Meijgaard (2008) although their analysis may be sensitive to the transition from large-scale to convective rainfall in hourly data (Haerter & Berg 2009). A super-thermodynamic response is also at odds with climate change scalings described by O'Gorman & Schneider (2009). Although the effect of large spatial reorganisation of circulation systems associated with El Niño are reduced by considering wet regimes, it has yet to be demonstrated that interannual variability is a realistic surrogate for climate change.

Some of the model simulations display a relationship between precipitation extremes and warming that is close to the observations although there is a large spread; previous work has noted the substantial sensitivity of tropical precipitation to changes in vertical motion within such events (Gastineau & Soden 2009, O'Gorman & Schneider 2009), likely to relate to differences in model parametrizations. With improved homogeneity of the satellite data it will be informative to analyse trends in precipitation extremes with warming.

In summary, positive trends in the wet regions and negative trends in the dry regions of the tropics are consistent with but smaller than previous analysis (Allan & Soden 2007) and closer to model simulations. The sensitivity of the observed results to the time-period and region chosen and the dataset employed shows the need for further improvements in the inter-calibration and homogenisation of datasets and continued inter-comparisons of different products, for example from the Tropical Rainfall Measurement Mission (John et al. 2009). Finally, a good physical understanding of the relationships between energy entering and stored in the climate system and the global water cycle are vital in predicting and planning for global change (Trenberth 2009, Stephens & Ellis 2008, Wild et al. 2008).

Acknowledgments

RPA was supported by NERC grants NE/C51785X/1 and NE/G015708/1. The Met Office contribution was supported by the U.K. Joint DECC and DEFRA Integrated Climate Programme - GA01101. We thank two annoymous reviewers for comments leading to improvments in the analysis. GPCP data were extracted from precip.gsfc.nasa.gov and the SSM/I data from www.ssmi.com. We acknowledge the modeling groups, the Program for Climate Model Diagnosis and Intercomparison and the World Climate Research Programme's Working Group on Coupled Modelling for their roles in making available the WCRP CMIP3 multi-model dataset. Support of this dataset is provided by the Office of Science, U.S. Department of Energy.

References

Adler R F, Gu G, Wang J J, Huffman G J, Curtis S & Bolvin D 2008 *J. Geophys. Res.* **113**, D22104+.

Allan R P & Soden B J 2007 *Geophys. Res. Lett.* **34**, L18705.

Allan R P & Soden B J 2008 *Science* **321**, 1481–1484.

Allen M R & Ingram W J 2002 *Nature* **419**, 224–232.

Chou C, Tu J & Tan P 2007 *Geophys. Res. Lett.* **34**, L17708.

Field P R & Shutts G J 2009 *Quart. J. Roy. Meteorol. Soc.* **135**, 175–186.

Gastineau G & Soden B J 2009 *Geophys. Res. Lett.* **36**, L10810.

Haerter J O & Berg P 2009 *Nature Geoscience* **2**, 372–373.

Held I M & Soden B J 2006 *J. Climate.* **19**, 5686–5699.

John V O, Allan R P & Soden B J 2009 *Geophys. Res. Lett.* **36**, L14702.

Kalnay E, Kanamitsu M, Kistler R, Collins W, Deaven D, Gandin L, Irdell M, Saha S, White G, Woollen J, Zhu Y, Chelliah M, Ebisuzaki W, Higgins W, Janowiak J, Mo K C, Ropelewski C, Wang J, Leetmaa A, Reynolds R, Jenne R & Joseph D 1996 *Bull. Amer. Met. Soc.* **77**, 437–471.

Lambert H F & Webb M J 2008 *Geophys. Res. Lett.* **35**, L16706+.

Lenderink G & van Meijgaard E 2008 *Nature Geoscience* **1**.

Liepert B & Previdi M 2009 *J. Climate* **22**, 3156–3166.

Liu S C, Fu C, Shiu C, Chen J & Wu F 2009 *Geophys. Res. Lett.* **36**, L17702.

Meehl G, Stocker T, Collins W, Friedlingstein P, Gaye A, Gregory J, Kitoh A, Knutti R, Murphy J, Noda A, Raper S, Watterson I, Weaver A & Zhao Z C 2007 Climate Change 2007: The Physical Science Basis. Contribution of Working Group I to the Fourth Assessment Report of the Intergovernmental Panel on Climate Change Cambridge University Press, Cambridge, United Kingdom and New York, NY pp. 747–845.

Mitchell J, Wilson C A & Cunnington W M 1987 *Quart. J. Roy. Meteorol. Soc.* **113**, 293–322.

O'Gorman P A & Schneider T 2009 *Proc. Nat. Acad. Sci.* **106**, 14773–14777.

Pall P, Allen M R & Stone D A 2007 *Climate Dynamics* **28**, 351–363.

Rayner N A, Parker D, Horton E, Folland C, Alexander L, Rowell D, Kent E & Kaplan A 2003 *J. Geophys. Res.* **108**, 4407.

Stephens G L & Ellis T D 2008 *J. Climate* **21**, 6141–6155.

Trenberth K E 2009 *Curr. Opin. Environ. Sustainability* **1**, 19–27.

Turner A G & Slingo J M 2009 *Atmos. Sci. Lett.* **10**, 152–158.

Uppala S M, Kallberg P W, Simmons A J, Andrae U, da Costa Bechtold V, Fiorino M, Gibson J K, Haseler J, Hernandez A, Kelly G A, Li X, Onogi K, Saarinen S, Sokka N, Allan R P, Andersson E, Arpe K, Balmaseda M A, Beljaars A C M, van de Berg L, Bidlot J, Bormann N, Caires S, Chevallier F, Dethof A, Dragosavac M, Fisher M, Fuentes M, Hagemann S, Holm E, Hoskins B, Isaksen L, Janssen P A E M, Jenne R, McNally A P, Mahfouf J F, Morcrette J J, Rayner N A, Saunders R W, Simon P, Sterl A, Trenberth K E, Untch A, Vasiljevic D, Viterbo P & Woollen J 2005 *Quart. J. Roy. Meteorol. Soc.* **131**, 2961–3012.

Vecchi G A, Soden B J, Wittenberg A T, Held I M, Leetmaa A & Harrison M J 2006 *Nature* **441**, 73–76.

Wentz F J, Ricciardulli L, Hilburn K & Mears C 2007 *Science* **317**, 233 – 235.

Wilcox E M & Donner L J 2007 *J. Climate* **20**, 53–69.

Wild M, Grieser J & Schär C 2008 *Geophys. Res. Lett.* **35**, L17706+.

Yang H & Tung K K 1998 *J. Climate* **11**, 2686–2697.

Zhang X, Zwiers F W, Hegerl G C, Lambert F H, Gillett N P, Solomon S, Stott P A & Nozawa T 2007 *Nature* **448**, 461–465.